Evaluation of the ESRO IV Satellite Horizon Crossing Indicator Performance

M.J. Brewer*
British Aircraft Corporation, Bristol, England
and
J. Soubirou†
European Space Research and Technology Centre, Noordwijk, The Netherlands

The ESRO IV satellite Horizon Crossing Indicator performance was derived from the ground-processing of flight data, using the Kalman filtering technique and the comparison of simulated and telemetered sensor data. It is shown how the effect of inherent sensor triggering delays were reduced by in-orbit calibrations, in the presence of partially known parameters of the measurement process. Typical in-orbit calibration curves are presented for a range of satellite altitude, crossing obliqueness and spin rates. The standard deviation of the sensor noise and the statistical uncertainty of the in-orbit calibration were examined to evaluate the attitude sensor accuracy. Satellite attitude histories, with an accuracy better than 0.5° and an estimation of the principal axis tilt, were derived from the attitude sensor data.

I. Introduction

THE ESRO IV[1] satellite, which was launched in November, 1972, carried five scientific experiments for in vestigation of neutral and ionized particle species, and densities in the ionosphere and near magnetosphere, and the flux energy and pitch-angle distribution of auroral particles, together with a technological experiment.

The objective of the experiment is to space-qualify an infrared Earth Horizon Crossing Indicator (HCI). References 3 and 4 describe the main aspects of the system analysis, design, and testing of the instrument which was developed under the responsibility of the European Space Research and Technology Centre (Noordwijk aan Zee, The Netherlands). The space qualification results from the evaluation of the in-orbit performance of the attitude sensor which is measured by: 1) the accuracy with which it is able to detect the Earth's horizon; 2) its suitability for attitude reconstitution of spinning satellites; and 3) the comparison of predicted and in-orbit sensor data.

The inherent HCI triggering delays and the HCI sensing accuracy are statistically obtained via the ground-processing of the HCI in-orbit data, using the Kalman filtering technique without the use of an independent attitude measuring system. In addition, ESRO IV attitude histories and an estimate of the ESRO IV principal axis tilt are extracted from the HCI data, using the same computer program. The HCI in-orbit data are finally compared with those generated by a simulation of the complete HCI measurement process which was used to develop and test the Kalman Filter computer program.

II. ESRO IV Satellite and Mission

The mass of the ESRO IV satellite[1] is approximately 115kg and it is spinstabilized with an initial spin rate after the boom deployment of 66 rpm. Since there is no spin-up system, the spin rate will decrease to about 40 rpm after 18 months. The orbit is polar with apogee and perigee altitudes at injection equal to 1180 km and 250 km, respectively. The chosen orbit results in a perigee precession rate of approximately +3.5° per day, but the orbit plane remains approximately fixed in inertial space. To meet the scientific experiment requirements, attitude maneuvers are performed by a magnetic control system, based on the quarter orbit timer principle.

The operational attitude measuring system comprises a digital sun sensor and a tri-axial magnetometer. The sun sensor, which measures the angle between the satellite-sun vector and the satellite spin axis, has command reticle slits parallel to the spin axis, so that a sun reference pulse occurs when the sun is contained in the command reticle plane. The spin rate is derived from the information contained in the AURORA system telemetry data.[2]

III. HCI Description and Operation

The HCI is a pencil sensor with a field of view of 3° square and is mounted on the satellite so that its optical axis is approximately perpendicular to the satellite geometric spin axis. The HCI may be split into two main blocks; an optical system, which picks up the earth's infra-red radiation and an electronics box, which processes the input radiation to indicate the two earth horizons (i.e., space/earth and earth/space horizons).

The optical system consists of a Germanium lens, which focuses the input radiation onto a detector which is a Ge-immersed thermistor bolometer. Between the lens and the detector there is a filter which limits the radiation to the 14-16.25μ wavelength band. The radiation falling on the bolometer sensitive element alters its resistance and a voltage, which is directly proportional to the input radiation, is generated across the bridge. The thermal capacity of the bolometer introduces a 2.5 ms lag to the signal.

The electrical signal is fed through a preamplifier and a high pass filter. This produces signal responses at each horizon once in every spin period. The peak values of the responses are stored on two peak detectors and the next horizons are indicated when the response exceeds 50% of the previous peak value. A pulse is generated when each of the horizons is indicated, and these pulses are used in one of the two following modes.

If the satellite is in sunlight, a sun reference pulse is generated when the sun enters the field of view of the command reticle of the sun sensor. This pulse is used to start two counters driven by a very accurate high frequency clock. The first of these counters is stopped by the pulse indicating the space/earth horizon and the second by the earth/space pulse.

Received June 10, 1974; revision received October 7, 1974.
Index categories: Spacecraft Attitude Dynamics and Control; Spacecraft Flight Testing.

*Systems Engineer, Systems Technology Department.
†Design Engineer, Control and Stabilization Division; presently with Engins Matra, Velizy, France.

From the two counter values and the spin rate, the angles from the sun to the earth's horizons are derived.

If the satellite is in eclipse, the first counter is started by the space/earth crossing and stopped by the earth/space crossing; inversely, the other counter is started by the earth/space crossing and stopped by the space/earth crossing.

IV. Problem Statement

Of primary concern in this evaluation is the HCI accuracy in sensing the earth's infra-red transition and its suitability as an instrument for satellite attitude reconstitution in an inertial co-ordinate system. An idealized instrument for satellite attitude reconstitution would detect the earth's physical horizon. However, in the real situation, the earth pulses generated by the HCI do not correspond to the crossing of the earth's physical horizon by the HCI optical axis. The inherent HCI triggering delay is defined to be the time interval or the azimuth separation angle between the ideal earth pulse (physical horizon) and the real earth pulse generated by the HCI. When an estimate of the HCI scanning motion in inertial space and a mathematical model of the HCI response are available, the major part of the inherent HCI triggering delay is predictable. In fact, the HCI sensing error is defined to be the sum of a random error (zero mean) and a systematic error which represents the error in estimating the inherent HCI triggering delay. In view of the lack of an independent attitude measuring system with an accuracy better than the one of the HCI, a direct evaluation of the HCI sensing error and of the accuracy of the satellite attitude re-constitution on the basis of the HCI in-orbit was not feasible. However, Kalman Filtering applied to the HCI in-orbit data provides an estimate of the inherent HCI triggering delays. The variation in the estimated delays will represent a measure of the HCI systematic sensing error. In addition, the satellite attitude reconstitution accuracy may be derived in a statistical manner from the Kalman Filter covariance matrix or by examining the variations between test cases.

V. Inherent HCI Triggering Delays

The inherent HCI triggering delays originate from three categories of delay sources: 1) delays inherent in infra-red horizon sensing; 2) delays due to the method of locating the earth's horizon; and 3) delays in implementing the method. The two major inherent delays in infra-red horizon sensing are due to earth's oblateness and horizon displacement. The former is significant for the ESRO IV orbit, but is completely known. The horizon displacement error refers to the fact that the earth's "infra-red" horizon is some 35-40 km above the earth's physical horizon and the transition from zero radiance to maximum is spread out over approximately 50 km.

The method used to locate the earth's horizon introduces significant inherent HCI triggering delays. The optical integration of the IR radiance profiles in the HCI field of view and the electronic lags of the bolometer, high-pass and low-pass filters are such that the HCI triggers at about 15 km and 65 km above the earth's surface for the space/earth and earth/space crossings, respectively. In particular, the integrated infra-red profile is strongly dependent upon the satellite altitude, the satellite spin rate, and earth aspect angle, and to a lesser extent, on the angle at which the optical axis of HCI approaches the earth's surface.

The final category of delay originates from the implementation of the measurement process. Bolometer random noise and those HCI parameters subject to in-orbit changes, (such as alignments, or signal processing time constants) are delay sources due to the HCI itself. In addition, satellite system parameters which are partially known contribute to the estimates of the inherent HCI triggering delays. Examples of these are satellite principal spin axis tilt, satellite position vector, spin rate, sun reference pulse, and satellite nutation.

VI. Kalman Filter Model

The estimation algorithm used for the evaluation of the in flight performance of the HCI was the extended Kalman filter. In this the propogation of the linearization errors due to a poor initial estimate of the state is greatly reduced by relinearising the measurement equations about the current state estimate. For the evaluation of the HCI the implementation of the algorithm was straightforward, the major area of interest being the choice of the measurement and state vectors.

A. Measurement Vector

The HCI measurements, which are telemetred back from the satellite for possible use in the Kalman filter model, are the bolometer temperature, the space/earth peak level, the earth/space peak level, the sun-space/earth counter, and the sun-earth/space counter. Ideally, it is advantageous to use all available information for evaluation of the HCI in-orbit performance. However, analytical investigations show that the bolometer temperature has very little effect on the HCI characteristics and that the peak levels are strongly dependent on the earth's infra-red radiance profile variations and uncertainties. Therefore, the measurement vector chosen was simply the two HCI counter values corresponding to the sun-space/earth horizon and the sun-earth/space horizon angles.

B. State Vector

The choice of suitable elements for the state vector is governed by two important criteria. The first of these is that the change in any element must have a significant effect on the measurements, otherwise, it will be impossible to obtain a better estimate than that measured on the ground. The second criterion is that each element must be separately "observable" from the measurements. This, therefore, excludes the estimation of those parameters whose variations have precisely the same effect on the measurements.

The first two elements which must be included in the state vector are two angles which represent the satellite attitude in an inertial coordinate system. The two attitude angles, ξ and η, are right ascension and declination angles measured from the initial nominal spin axis orientation.

The largest source of inherent HCI triggering delay comes from the method of location of the earth's horizon. The triggering delay in the earth/space horizon can be as large as 3°. Provided that a mathematical model is available to predict the HCI response, the obvious approach is to try to estimate parameter(s) associated with the earth's radiance profiles, therefore eliminating some of the uncertainties associated with the triggering delays. In Fig. 1, a typical integrated radiance profile is shown, and it will be noted that it approximates very closely to a linear ramp followed by a constant value. If the earth's radiance profile had been a step function rather than a continuous curve, an actual linear

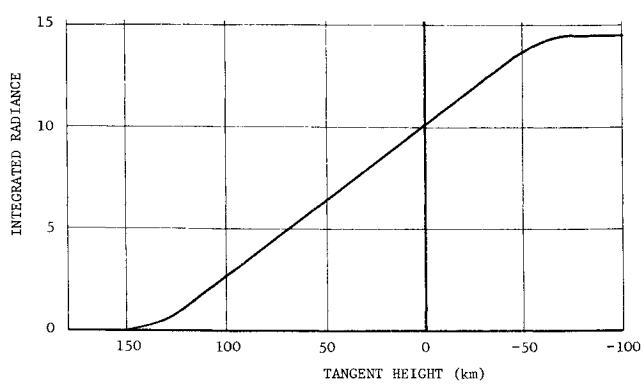

Fig. 1 Typical integrated radiance profile.

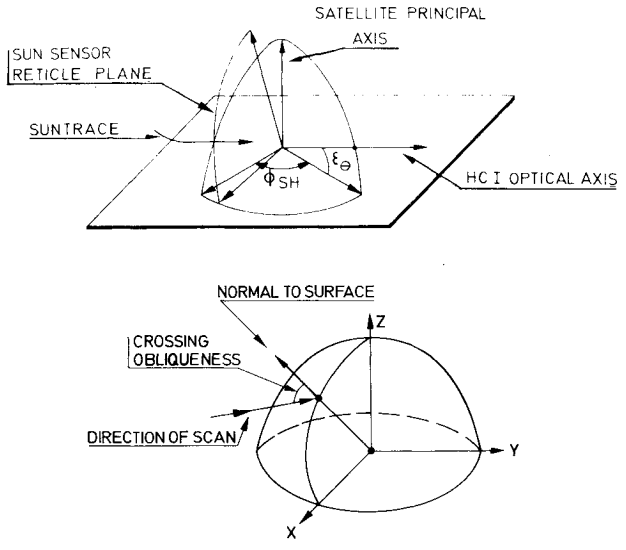

Fig. 2 Definition of main measurement process angles.

ramp would be obtained with the 50% point corresponding to the tangent height at which the step function is located. Therefore, the tangent heights, h_{T01} and h_{T02} of the two step functions corresponding to the space/earth and earth/space infra-red horizons were incorporated in the state vector.

The final two elements of the state vector are the effective azimuth separation angle ϕ_{SH} between the sun sensor command reticle plane/HCI optical axis and the effective HCI optical axis elevation angle ϵ_θ. These two elements which are shown in Fig. 2, combine several effects: satellite principal axis tilt, sun reference pulse error, and alignment errors. For the small segments of orbits likely to be used for the estimation, the state vector can be assumed to be constant, so that the transition matrix is simply the identity matrix.

C. The Measurement Equation and Implementation

The measurement equation was expressed in the following form:

$$\Phi_i = \Phi_{Ni} + \Phi_{SH} + \Phi_{BTi} + \Phi_{ENC} + \Phi_{\text{noise}}$$

$i = 1$ refers to the space/earth crossing; $i = 2$ refers to the earth/space crossing; Φ_{Ni} are the nominal HCI angles assuming that the HCI triggers at the earth's physical horizon. They include the effects of earth's oblateness and the component of satellite principal axis tilt in the meridian plane containing the HCI optical axis (ϵ_θ); Φ_{SH} is the effective azimuth separation between the HCI and the sun sensor command reticle; Φ_{ENC} is the mean of the error due to the encoding process; Φ_{noise} is the random noise resulting from sensor noise and digitization; and Φ_{BTi} are the systematic parts of the inherent HCI triggering delays due to the method of location of the horizon. They represent the in-orbit calibration of the HCI.

The Φ_{BTi} angles are analytically calculated with the assumption that the rate of change of tangent height with time is linear. The approximation is realistic when the crossing obliqueness (Fig. 2) is close to zero, but becomes less valid as the crossing obliqueness increases. Figure 3 shows the errors associated with this simplification for increasing obliqueness. It was decided that a maximum error of 0.1° was acceptable and, therefore, the processing of HCI in-orbit data was restricted to measurements corresponding to crossing obliquenesses up to 40.°

A computer program corresponding to the described Kalman Filter model was developed. The program requires 128 Kbytes and a CPU time of 3 min on an IBM 370/145 for a pass of 100 HCI measurements.

VII. System Observability Analysis

When estimating the state vector of a dynamic system, the statistical accuracy of the resulting estimate is limited by the basic observability of the system. The observability is a function of the state transition matrix, the measurement matrix and covariance of the measurement noise.

Observability problems arise if the dimension of the state vector is large compared with the dimension of the total observation vector (i.e., dimension of the measurement vector x number of observations) or if the transition matrix is close to unity and the measurement matrix slowly varying compared with the sample rate. The precise mathematical formula relating the observability is given in Part 2, Sec. 6 of Ref. 5 and its relationship with the filter covariance matrix is discussed. It is concluded that the observability of the system can be investigated by considering the filter covariance matrix without the a priori information. This is the approach adopted in the HCI observability study. The observability of chosen blocks of 100 observations covering a range of crossing obliquenesses was compared for each of the four planned attitudes for the first six months. The major conclusions of the observability study are as follows: 1) The observability of the system increases with crossing obliqueness. This effect is, however, offset by the increase in system error with obliqueness as shown in Fig. 3. 2) The best results are obtained when the spin axis is not in the orbit plane.

The reason for this result can be seen by examining the information contained in one set of HCI measurements. From combinations of them and a knowledge of the satellite position vector the earth aspect angle and the sun-earth azimuth angles can be calculated. Let us consider reconstitution of the satellite spin axis from the aspect angles only for a series of satellite position vectors around the orbit. If the spin axis is in the orbit plane the reconstitution is given by the contact line of two touching cones which therefore gives poor accuracy. However, if the spin axis does not lie in the orbit plane, the cones become intersecting; hence greatly improving the accuracy of the system. The observability of the system is also affected by the position of the sun, since colinearity of the earth-center, satellite, and sun will also give poor observability.

VIII. Kalman Filter Performance

A. Examination of Raw HCI In-Orbit Data

Examination of the HCI in-orbit data for the first 6 months after launch shows that there are six long periods where the satellite attitude is fixed, apart from a slight drift due to the perturbing torques. The timescales of these attitudes (designated A1-A6) and the maneuvers in between (M1-M5) are given in Table 1.

Examination of the HCI counter values revealed two interesting features. The first of these was the almost completely smooth nature of the values, as a function of time,

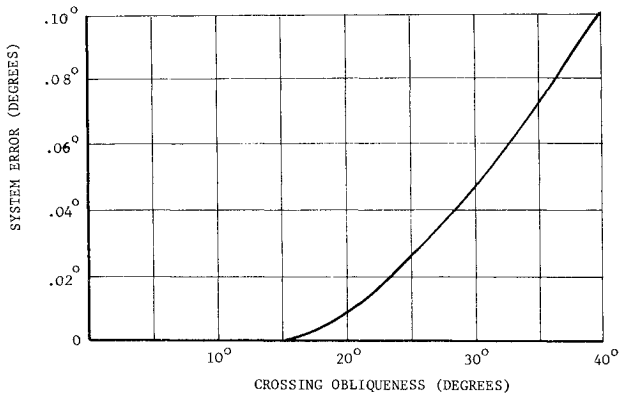

Fig. 3 System error due to the simplified HCI model.

Table 1 Nominal ESRO 4 spin axes orientations

State	Modified Julian dates(1950)	Right ascension	Declination
Attitude 1	8360—8367	288°	—70°
Maneuver 1	8368—8372	. . .	. . .
Attitude 2	8372—8388	309°	9°
Maneuver 2	8388—8393	. . .	. . .
Attitude 3	8393—8424	200°	8°
Maneuver 3	8424—8428	. . .	. . .
Attitude 4	8428—8469	112°	—33°
Maneuver 4	8469—8479	. . .	. . .
Attitude 5	8479—8494	290°	2°
Maneuver 5	8494—8497	. . .	. . .
Attitude 6	8497—8535	265°	84°

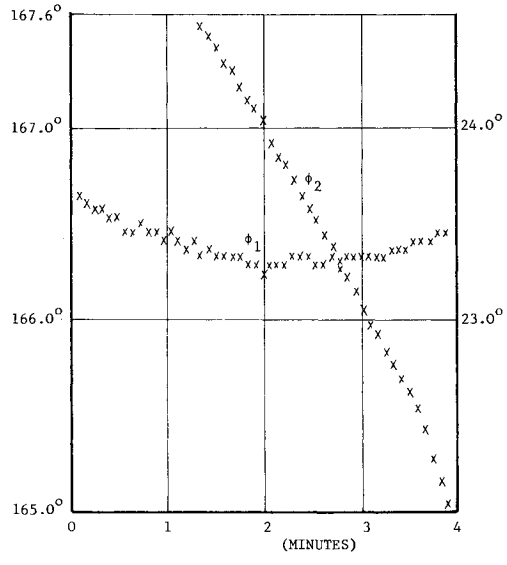

Fig. 4 Typical HCI traces (Attitude 6).

throughout the six months. This is illustrated in Fig. 4, which shows typical traces for attitude 6. It will be seen from the diagram that the fluctuations are little greater than the encoding error (±0.02°). This indicates that there is no nutation of the spin axis. The other interesting feature was that there is a deadband in the sensor operation so that if the value of a counter is within 18 msec of the spin period, the counter registers zero. This restricts the useful data to the range 0° to 353° for each angle. As the satellite spins down this range is slowly increased.

B. Choice of Key Kalman Filter Parameters

Three parameters which affect the accuracy of the state vector estimation are the duration of the period over which data are filtered, the time step between filtering measurements, and the amount of measurement noise. From examination of the state vector covariance matrix, it was found that the observability quality is largely improved as the observation period is extended, particularly for the biases (Φ_{SH} and ϵ_θ) and the tangent heights (h_{T01} and h_{T02}). However, this is to some extent offset by the fact that filtering over the larger arc introduces larger variations in the radiance profile parameters (h_{T01} and h_{T02}).

The second parameter of major importance was the time step between observations. It was noted from examination of the raw sensor data, that the Kalman filter is really estimating parameters rather than filtering out noise. The important parameter is, therefore, the change in geometry rather than the number of measurements. The philosophy used in the comprehensive processing of in-orbit data was, therefore, to filter over large arcs of the orbit, (i.e., one fifth of an orbit period), using a maximum of 100 observations and adjusting the time between observations as appropriate.

Table 2 Typical measurement residuals (Altitude 4)

ΔØ1 (deg)	ΔØ2 (deg)
—0.05	0.09
—0.01	0.04
0.00	—0.02
—0.01	0.02
0.01	0.02
0.03	0.00
0.02	0.02
—0.04	0.02
—0.01	0.03
—0.01	—0.04
—0.04	—0.04
—0.04	0.00
—0.01	0.03
0.00	0.05
—0.02	0.01
—0.05	—0.02
—0.06	—0.01
—0.02	0.00
—0.06	—0.01

It was noted from the smoothness of the HCI measurements that there was not nutation and very little noise. It was, therefore, decided to use a measurement noise standard deviation of 0.03° for the major processing of the data. However, it was stated previously that there is a system error introduced in the filter which increases with crossing obliqueness, particularly above 30°. The size of the measurement noise was, therefore, increased linearly above 30° so that it was doubled for an obliqueness of 40°.

To test the suitability of the level of the measurement noise, a typical filter run was considered for attitude 4 to examine the residuals. The latter are the angular differences, at each step, between the real data and the corresponding filter measurements and reflect the level of the random noise and the satisfactory operation of the filter. The values of the residuals are given in Table 2, and it can be seen that the standard deviation is close to 0.03°, thus, illustrating the suitability of the original choice.

C. Kalman Filter Test Cases

The convergence properties of the Kalman filter were tested for a typical case for attitude 5. The convergence was tested by processing the same data four times, but with widely differing initial conditions. The results of filtering 100 observations over a large arc with 12 sec between observations are shown in Figs. 5 and 6, which show the angular biases and the radiance profile parameters, respectively. For convenience, only every tenth value is plotted. The convergence of the filter, for the widely different initial conditions, is excellent as was predicted by the a priori observability study.

Table 3 illustrates the consistency properties of the Kalman filter. Three cases were selected over two consecutive orbits. The consistency of the attitude angle estimates is better than 0.2° between two passes made up of apogee data and better than 0.3° between two passes made up of apogee and perigee data. Figure 7 illustrates the stability of the Kalman filter and the variation of the standard deviations of the state vector elements.

IX. HCI In-Orbit Calibration

The values of the two estimated inherent triggering delays ϕ_{BT1} (space/earth horizon) and ϕ_{BT2} (earth/space horizon)

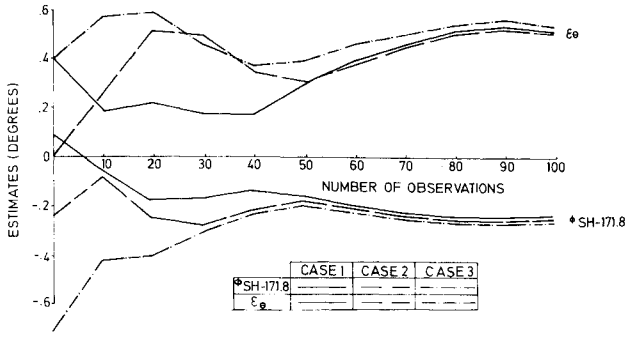

Fig. 5 Convergence test case— Φs_h and ϵ_θ estimates.

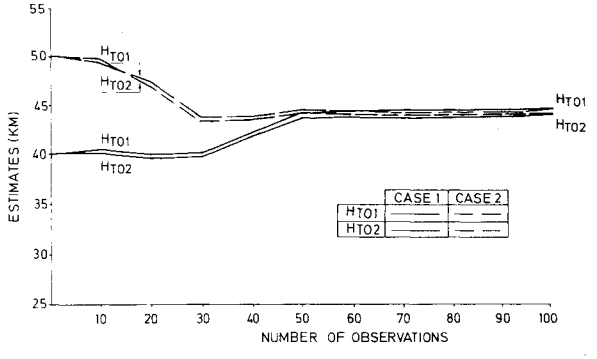

Fig. 6 Convergence test case—h_{TO1} and h_{TO2} estimates.

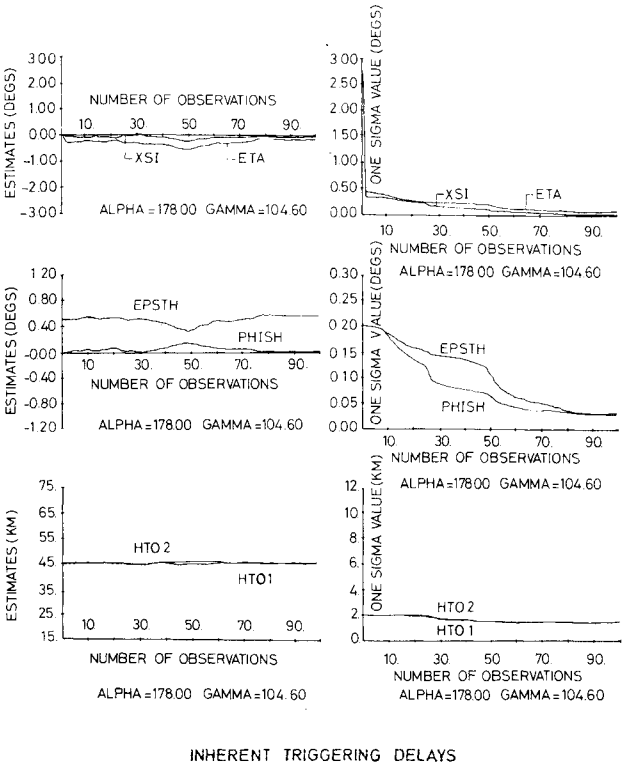

Fig. 7 Stability test case—Evolution of estimates and standard deviations.

are basically a function of five quantities. These are satellite altitude and spin rate, crossing obliqueness of the optical axis, latitude of the horizon, and time of year. To find comprehensive values of the calibration angles is impossible since, for instance, the spin rate does not vary independently of the time of year. The last two parameters given only affect the calibration curves through variation in the earth's radiance profiles which is a relatively small effect. Figures 8 and 9 show the inherent triggering delays for crossing obliqueness of 0° and 35° respectively. The standard deviations associated with the curves which are calculated from the state vector covariance matrix for zero crossing obliqueness is less than 0.05°.

This is consistent with variations between cases. For the larger crossing obliqueness (35°), the standard deviations from the filter are up to 0.07°. The fluctuations in the curves indicate, however, that a more realistic value is 0.1°. These fluctuations might be due to the introduction of increasing system errors for larger crossing obliqueness.

X. Simulation Tests

During the course of the Kalman filter program development, "pseudo-real" HCI measurements were generated, using a detailed simulation of the satellite orbit and attitude dynamics and the measurement process. To evaluate the consistency between the real and simulated measurement process,

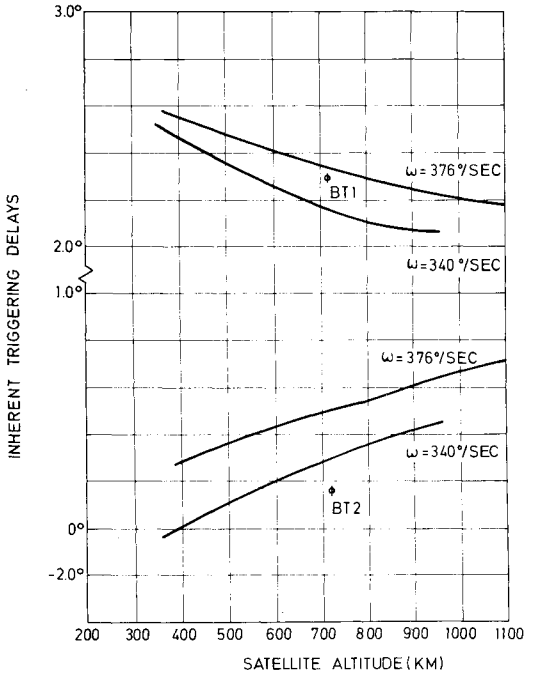

Fig. 8 Inherent triggering delays (zero obliqueness).

Table 3 Consistency test results

Orbit number	Altitude (km)	Crossing obliqueness (deg)	Final estimates of state vector: Right ascension (deg)	Declination (deg)	$\emptyset_{SH}$ (deg)	ϵ_Θ (deg)	h_{TO1} (km)	h_{TO2} (km)
1741	800—1000	<40°	290.63	2.13	171.38	0.53	45	46
1742	800—1000	<40°	290.76	2.05	171.41	0.60	45	46
1741	285—240	<20°	290.58	2.20	171.28	0.39	40	40

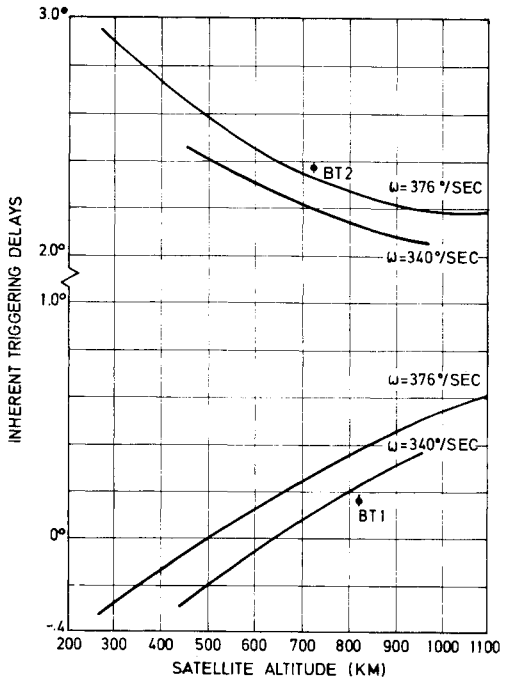

Fig. 9 Inherent triggering delays (obliqueness 35°).

the outputs from five suitable filter runs were fed into the simulation and the corresponding HCI angles and peak values calculated.

For each attitude, five measurements were considered corresponding to different satellite radius vectors spread around the arc of the orbit. These cases cover a wide variation of all the important parameters which affect the HCI measurements i.e. satellite altitude and spin-rate, crossing obliqueness of the optical axis, latitude of the horizon, and time of year. To eliminate the possibility of introducing unnecessary errors due to the orbit model, the model was changed so that the radius vectors derived from tracking data are used directly. The consistency for the HCI angular measurements is in general very good, 70% of the simulated values being within 0.03° of the real values. The consistency of the peak values is also good, particularly for attitudes 3, 4, 5, and 6, where the simulated values are all within 5% of the real ones. The simulated peak values for attitude 2 are, however, up to 18% lower than the real peak values. It should be noted that the cases considered for attitude 2 are all close to the South pole at mid-summer for the southern hemisphere. The radiance profile curves used for the simulation were for the northern hemisphere only, and the southern hemisphere was taken to be a "mirror image" of it. It was also noted from Ref. 6 that the uncertainty in the maximum radiance values is greatly increased during the summer, particularly for the larger latitude values. In view of this, it is considered that the simulated peak values for attitude 2 are quite acceptable.

XI. ESRO IV Attitude Histories

The Kalman filter program was primarily aimed at the evaluation of the HCI in-orbit performance. However, the program also estimates to a high degree of accuracy, the satellite attitude at any time assuming that it is fixed over the interval of filtering. The filter was, therefore, used to give a comprehensive attitude history for ESRO IV from December 12, 1972 to May 15, 1973. Although the Kalman filter makes no allowance for attitude dynamics, it was also used during maneuvers to give the complete attitude history.

The variation of the direction of the spin axis over the five month period is illustrated, using a polar spatial plot (Fig. 10), whereas Fig. 11, shows the attitude 5 history. During maneuvers, the covariance matrices indicate an attitude

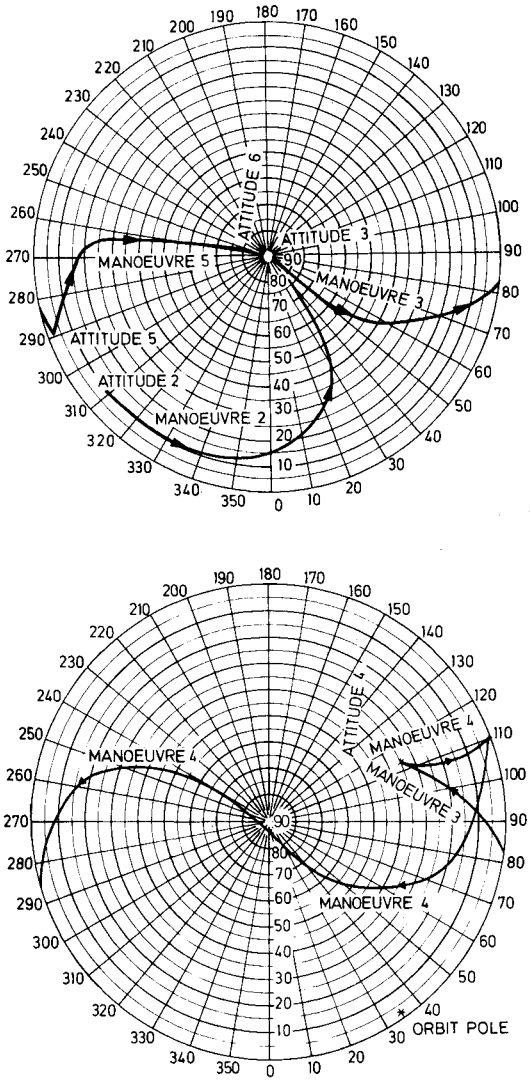

Fig. 10 a) Attitude history: Northern hemisphere. b) Attitude history: Southern hemisphere.

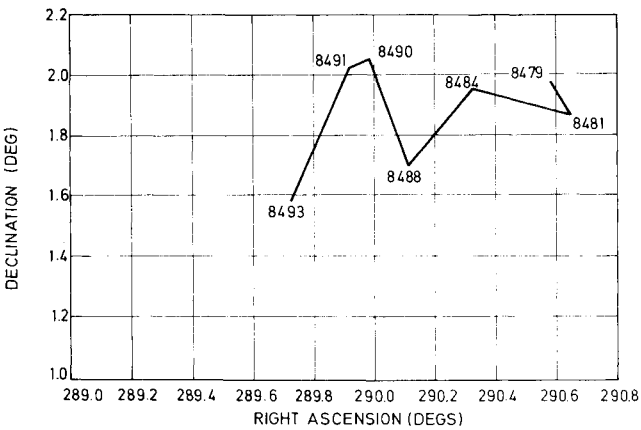

Fig. 11 Attitude 5 history.

reconstitution accuracy of the order of 0.3° (1σ). This is probably optimistic. The covariance matrices for the relatively fixed attitude give an attitude accuracy of approximately 0.2° (1σ). The fluctuations in the attitude history curves for different cases indicate a slightly higher value, although the maximum flunctuations are practially all less than 0.5°.

XII. Estimation of Satellite Principal Axis Tilt

From the estimates of the effective HCI optical axis elevation error (ϵ_θ) and the effective azimuth separation between the sun sensor command reticle and the HCI optical axis (ϕ_{SH}), the satellite principal axis tilt was calculated, using parameter estimation techniques, as described in Appendix 3 of Ref. 5 (Part III). The calculation pre-supposes that the sensors are perfectly aligned to the satellite geometrical axis and that the sun reference pulse has a constant calibration error. The magnitude of tilt was estimated to be 0.37° and the direction of tilt is in a meridian plane within 6° of the plane containing the HCI optical axis and is towards the optical axis. The associated standard deviation is approximately 0.16°.

XIII. Conclusions

From the results of the ground-processing performed using the HCI in-orbit data and the simulation of the measurement process, it is possible to make an assessment of the in-orbit performance of the HCI, for the first six months of its lifetime. A satisfactory assessment was found between the simulated measurements (based on estimated parameters and pre-launch test) and the real data, for both the counter values and the peak values.

The most important part of the space qualification of the HCI is its sensing accuracy (ability to sense the earth's horizon). The long time constants associated with the HCI electronics give an inherent triggering delay of up to 3° for the earth/space transition. This delay was reduced by in-orbit calibration of the sensor, using a mathematical model of the HCI and its electronics. The resultant sensing accuracy then depends only on the uncertainty of the in-orbit calibration and the noise associated with the sensor. The standard deviation of the latter is very small (approximately 0.02°). The accuracy of the in-orbit calibration depends upon the crossing obliqueness of the HCI sweep. For zero obliqueness, the standard deviation is less than 0.05°, but for an obliqueness of 35°, the standard deviation may be up to twice this value, particularly at the lower satellite altitudes.

In spite of a deadband which restricts the operating of each of the counters in such a way that the angles between 353° and 360° are not monitored, the use of the HCI as a basic attitude determination instrument was also demonstrated. The attitude accuracies achieved with a Kalman filter program, for the nonmaneuvering parts of the mission, are better than 0.5°.

A comparable accuracy would also be obtained during maneuvers by modeling the maneuvers in the system equation. From the HCI measurements, it was also possible to estimate the amplitude and phase of the satellite principal axis tilt.

References

[1]Lafay, J.F., "Le Satellite ESRO 4," *ELDO/ESRO Scientific and Technical Review,* Vol. 4, 1972, pp. 313-351.

[2]"General Description of the ESRO IV Satellite," E4/PD/10, Issue 3, Aug. 1972, European Space Research Organization, Noordwijk, The Netherlands.

[3]Menardi, A.S., "Horizon Crossing Indicator Technological Experiment on ESRO IV," Fourth Conference on Space Optics, Marseille, Nov. 6-8, 1973, pp.197-207.

[4]Baldassini-Fontana, R., De Vidi, G., Simoncini, G., "Horizon Crossing Indicator for ESRO IV Satellite," 255-DT-1, Nov. 1973, Officine Galileo, Florence, Italy.

[5]Brewer, M.J., Chesson, R., Moffatt, T., "Study and Evaluation of the ESRO IV Satellite Horizon Crossing Indicator In-Orbit Data," ESS/SS 364, ESS/SS 405, ESS/SS 533, British Aircraft Corporation, Bristol, U.K.

[6]Thomas, J.R., "The Analysis of 15μ Infra-Red Horizon Radiance Variations over a Range of Meteorological, Geographical and Seasonal Conditions," April 1967, CR 725, NASA.